International Journal of Concrete Structures and Materials
Vol.10, No.1, pp.29–37, March 2016
DOI 10.1007/s40069-016-0125-z
ISSN 1976-0485 / eISSN 2234-1315

# Tensile Properties of Hybrid Fiber-Reinforced Reactive Powder Concrete After Exposure to Elevated Temperatures

**Haiyan Li*, and Gang Liu**

(Received August 19, 2015, Accepted January 4, 2016, Published online January 25, 2016)

**Abstract:** The paper presents a research project on the tensile properties of RPC mixed with both steel and polypropylene fibers after exposure to 20–900 °C. The direct and the indirect tensile strength (in bending) were measured through tensile experiment on dog-bone specimens and bending experiment on 40 × 40 × 160 mm prisms. RPC microstructure was analyzed using scanning electron microscope. The results indicate that, steel fibers can significantly improve the tensile performance of hybrid fiber-reinforced RPC, whereas polypropylene fibers have no obvious effect on the tensile performance. With increasing temperature, the flexural and axial tensile strength of hybrid fiber-reinforced RPC substantially decrease linearly, which attributes to the deteriorating microstructure. Based on the experimental results, equations are established to express the decay of the flexural and tensile strength with increasing temperature.

**Keywords:** reactive powder concrete (RPC), tensile properties, elevated temperatures, steel fiber, polypropylene fiber, scanning electron microscope (SEM).

## 1. Introduction

The tensile properties of concrete after high temperature are very important for the evaluation of the residual behavior in tension of concrete structures after exposure to high temperatures (EN 1992-1-2 2004). Up to now, a lot of research on the residual mechanical properties of normal strength concrete (NSC) and high strength concrete (HSC) has been performed. It was found that the flexural strength and tensile strength of both NSC and HSC substantially decrease linearly with increasing temperature (Husem 2006; Khalig and Kodur 2011; Chang et al. 2006). Adding steel fibers to the concrete can effectively improve the tensile properties after exposure to high temperature (Song and Wang 2004), whereas the incorporation of polypropylene fibers has no obvious effect on the tensile properties (Xiao and Falkner 2006). The variations exhibited by the flexural strength for HSC with or without steel fibers and polypropylene fibers were explained by Pliya et al. (2011) Chen and Liu (2004) studied the effect of steel fibers, polypropylene fibers and hybrid fibers on the residual splitting tensile strength of HSC. Compared with plain concrete, the residual splitting tensile strength of HSC mixed with steel and polypropylene fibers improved significantly.

Mechanics Engineering Department, Shijiazhuang Tiedao University, Shijiazhuang 050043, People's Republic of China.
*Corresponding Author; E-mail: haiyan126@163.com
Copyright © The Author(s) 2016. This article is published with open access at Springerlink.com

The difference with NSC is that HSC is more prone to spalling when subjected to high temperature. Kodur (2000) considered that the low tensile strength and low porosity led to HSC spalling under the high temperature. Kalifa et al. (2000) found that the spalling probability of HSC improved under high temperature owing to its pore pressure being much higher than the NSC. The incorporation of steel fibers and polypropylene fibers can effectively reduce the occurrence of spalling. Han et al. (2005) discussed the influence of polypropylene fibers, metal fibers, carbon fibers and glass fibers on the spalling performance of HSC.

Reactive Powder Concrete (RPC) is an ultra high strength cement-based composite material made of ultra-fine reactive powder, cement, fine aggregate, high-strength steel fibers and other components (Richard and Cheyrezy 1995). It is a very promising building material in the field of civil engineering. Currently, many studies have been completed on the mechanical properties of RPC at room temperature, and the studies show that the mechanical properties of RPC are better than NSC and HSC (Yazıcı et al. 2010; Bayard and Ple 2003; Rashad et al. 2013). The steel fibers contained in RPC can greatly improve its tensile strength and toughness (Kang et al. 2010). Few studies have been performed on the mechanical properties of RPC after exposure to high temperature, especially on the tensile properties. Tai et al. (2011) showed that the mechanical properties of steel fiber-reinforced RPC increased firstly and then decreased with increasing temperature. Due to the elimination of the coarse aggregate, RPC has a denser internal structure than HSC (Cheyrezy et al. 1995; Li et al. 2012; Vance et al. 2014). Therefore, RPC is more prone to spalling than HSC under heating. The same with HSC, the incorporation of steel fibers and polypropylene fibers can also inhibit the spalling of RPC.

From above analysis it is found that the incorporation of steel fibers can obviously improve the mechanical properties of RPC, and the incorporation of polypropylene fibers have little effect on the mechanical properties, but can greatly reduce the damage extent of high-temperature to the specimen. When RPC mixed with both steel fibers and polypropylene fibers, on the one hand, the mechanical properties can be improved evidently, on the other hand, the high temperature spalling can be effectively suppressed.

For the abovementioned reasons, it is necessary to study the mechanical properties of RPC after exposure to elevated temperatures. A previous research (Zheng et al. 2012b) has discussed the compressive behaviour of hybrid fiber-reinforced RPC after exposure to high temperature. In this paper, in order to study the tensile properties of hybrid fiber-reinforced RPC after exposure to 20, 120, 200, 300, 400, 500, 600, 700, 800 and 900 °C, bending and direct tensile tests were carried out on 40 × 40 × 160 mm prisms and dog-bone specimens. The effects of fiber type, fiber content and temperature on the flexural strength and direct tensile strength are studied. The microstructure of RPC after different temperatures is studied using SEM test. Equations to express the decay of the flexural and direct tensile strength with temperature are proposed.

## 2. Experimental Program

### 2.1 Raw Materials and Mix Proportion

RPC was prepared on the basis of the following ingredients: ordinary Portland cement with Grade of 42.5 (Chinese cement grading system); silica fume with specific surface area of 20780 $m^2$/kg and $SiO_2$ mass fraction of 94.5 %; slag with the 28 days activity index of 95 % and specific surface area of 475 $m^2$/kg; quartz sand with $SiO_2$ mass fraction of higher than 99.6 %, and diameter range of 600–360 and 360–180 μm; concentrated naphthalene water reducer with form of brown powder; high-strength steel fiber with diameter of 0.22 mm and length of 13 mm; polypropylene fiber (PPF) with melting point of 165 °C and length of 18–20 mm.

Using above materials, the composition test on mix proportion was performed in advance, and the optimum mixture ratio was found out as: cement: silica fume: slag: quartz sand: water reducer: water = 1:0.3:0.15:1.2:0.058:0.29 (Li et al. 2010). Based on the optimum mixture ratio, through mixing different volume dosage of steel fiber and polypropylene fiber, three mix proportions (HRPC1, HRPC2 and HRPC3) are determined in this test, and the corresponding steel fiber and polypropylene fiber volume dosage are (2 %, 0.1 %), (2 %, 0.2 %) and (1 % 0.2 %), as shown in Table 1.

### 2.2 Specimen Design and Fabrication

The RPC preparation has to follow certain requirements. Firstly, the pre-weighed quartz sand, cement, slag, silica fume and water reducer were poured into concrete mixer and mixed for 3 min, then the pre-weighed water was poured into mixer and mixed for 5 min, next, the polypropylene fibers and steel fibers were poured into mixer and mixed for 5 min, finally, the mixture was poured into molds and vibrated on a high-frequency vibration table. After being stored for 1 day in the standard conditions, the specimens were demoulded and cured for 3 days at 90 °C in the concrete accelerated curing box. Next, the specimens were moved into a standard curing room and cured for 60 days. Before heating treatment, the specimens were taken out of standard curing room and exposed to air for 2 months.

Specimens used for the bending tests were 40 mm × 40 mm × 160 mm prisms; specimens used for the direct tensile test were dog-bone specimens, as shown in Fig. 1. According to the mix proportions in Table 1, for each mix proportion, ten groups of specimens were prepared. Each group consisted of three nominally identical specimens, a total of 180 specimens were prepared, and the final result is taken as the average of three test data.

### 2.3 High Temperature Tests

According to EN 1992-1-2 (2004), The high-temperature experiments were performed using an electric furnace once the specimens attained the required age, and ten reference temperatures were considered: 20, 120, 200, 300, 400, 500, 600, 700, 800 and 900 °C. The heating rate was 4 °C/min. The reference temperature was maintained for 2 h, so that the temperatures inside and outside of the specimen could be consistent. Through opening the furnace door, the specimens were cool down to room temperature. The temperature–time curves of the furnace for the different target temperatures are given in Fig. 2.

### 2.4 Bending and Tensile Tests Regime

The bending and tensile tests were carried out after the specimens were placed indoors for 3 days after high temperature tests. According to GB/T 17671 (1999), the bending tests were performed on a YAW-300 microcomputer automatic press-fold cement testing machine by self-made fixture, as shown in Fig. 3a. A steel bar with diameter of 10 mm was placed on the specimen surface in contact with the testing machine platen. The tests were controlled by load, and the loading rate was 0.5 kN/s. According to SL 352 (2006), the tensile tests were performed on a WDW3100 computer-controlled electronic universal testing machine through the pulling method with enlarging the specimen ends, as shown in Fig. 3b. The tests were controlled by displacement, and the loading rate was 0.5 mm/min.

### 2.5 Scanning Electron Microscope (SEM) Test

The microstructure of concrete after exposure to high temperature determines its macroscopic mechanical properties, so it is important to study the morphology and composition of RPC after elevated temperatures. In this paper, the samples used for SEM tests were taken from the specimens tested in direct tension, and exposed to 20, 200, 400, 600 and 800 °C. Zhou (2000) detailed description of the

**Table 1** Mix proportions of HRPC.

| Series | Binding materials (kg/m³) | | | Quartz sand (kg/m³) | Water reducer (kg/m³) | Water (kg/m³) | Steel fiber (%) | PPF (%) |
|---|---|---|---|---|---|---|---|---|
| | Cement | Silica fume | Slag | | | | | |
| HRPC1 | 799.72 | 239.92 | 119.96 | 959.66 | 46.38 | 231.92 | 2 | 0.1 |
| HRPC2 | 798.90 | 239.67 | 119.84 | 958.68 | 46.34 | 231.68 | 2 | 0.2 |
| HRPC3 | 807.07 | 242.12 | 121.06 | 968.48 | 46.81 | 234.05 | 1 | 0.2 |

Steel fibers and polypropylene fibers content are the volume dosage.

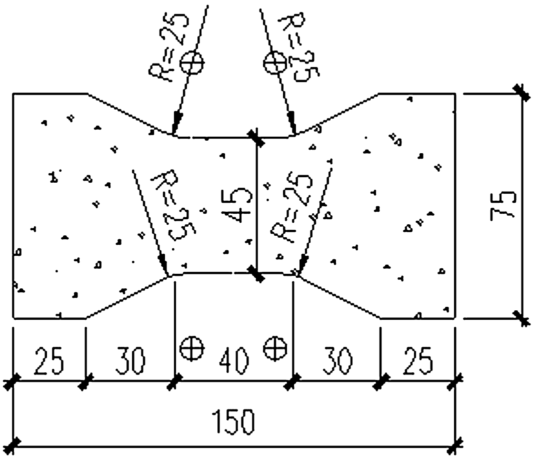


**Fig. 1** Dimensions of dog-bone specimen (Thickness of specimen: 45 mm).

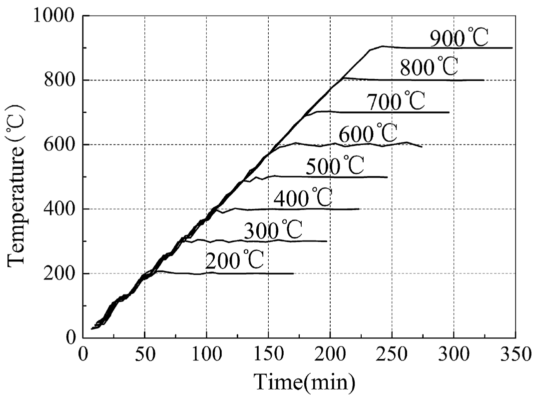


**Fig. 2** Temperature-time curves of the furnace for the different target temperatures.

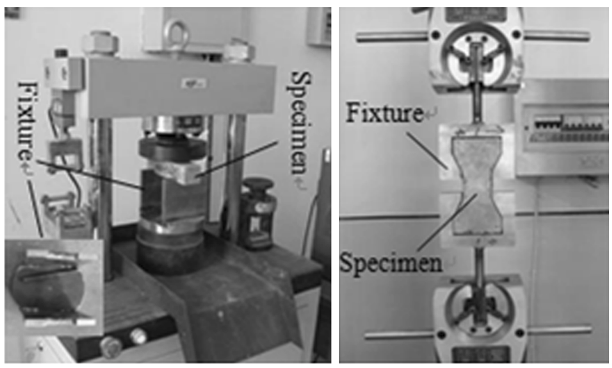


**(a)** Bending experiment **(b)** Tensile experiment

**Fig. 3** Loading devices for bending and tensile tests.

SEM test method. Firstly, small pieces of samples about 5 mm were prepared, then the small pieces were dried, vacuum pumped and sprayed-gold successively. Next, the microstructure of RPC matrix, bonding interface between steel fiber and matrix, PPF and PPF melting channel were photographed and observed using the Quanta200 scanning electron microscope.

## 3. Results and Discussions

### 3.1 Failure Modes of Specimen

#### 3.1.1 Flexural Failure Mode

Figure 4 shows the flexural failure modes corresponding to HRPC3 after exposure to elevated temperatures. With increasing load, a clear crack appeared first in the tension zone of the specimen. Meanwhile, the steel fibers crossing the crack came into play. As the load increased continually, the crack began to expand, meanwhile, the steel fibers constantly pulled out, and the load reached the maximum. Finally, the specimen damaged but did not break, and the failure mode presented obviously toughness when the temperature is lower than 700 °C. When the temperature is higher than 700 °C, the steel fibers lost effect, and the failure mode turned brittle.

#### 3.1.2 Tensile Failure Mode

The tensile failure modes of HRPC2 are shown in Fig. 5. All specimens of RPC corresponding to different mix proportions are pulled off along the cross-section of specimen with only one main crack. The bonding effect between the fibers and the matrix are destroyed gradually with the crack expanding. The steel fibers distribution on the crack is uneven and interlocked, and the steel fiber ends are still embedded in the RPC matrix. For temperatures below 700 °C, the steel fibers work effectively, and its incorporation improves the toughness of RPC, so the tensile failure mode is ductile failure. Beyond 700 °C, the carbonization of steel fibers occurs, and the steel fibers in RPC lose effectiveness, which increase the brittleness of RPC, so the failure mode converts to brittle.

As can be seen from the previous discussion, the ductility and toughness of RPC gradually improves with increasing steel fiber content. The interlocked distribution of the steel fibers is the main reason for RPC failure modes shifting from brittle to ductile.

**Fig. 4** Flexural failure modes of HRPC after elevated temperatures.

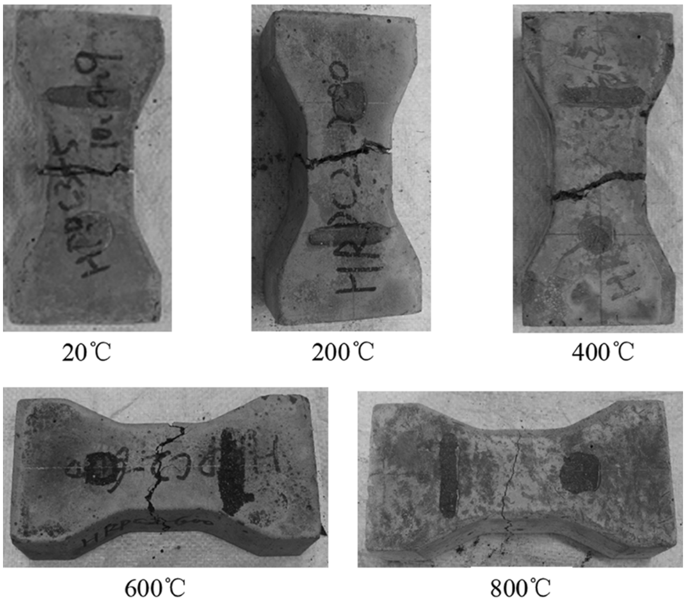


**Fig. 5** Tensile failure modes of HRPC after exposure to elevated temperatures.

### 3.2 Flexural Strength

The absolute and relative values of flexural strength for HRPC after different temperatures are given in Fig. 6. As seen from Fig. 6a, the flexural strength decreases gradually with increasing temperature, and the flexural strength of HRPC1, HRPC2 and HRPC3 reduces to 22.74, 24.55 and 19.28 % after 900 °C of the value at room temperature. For the same heating treatment, the residual flexural strength of HRPC1 and HRPC2 with the same steel fiber content of 2 % has almost no difference, but is much larger than HRPC3 with steel fiber content of 1 %, which means that the steel fibers can effectively improve the flexural strength of RPC after exposure to high temperature. On the contrary, PPF has little effect on improving flexural strength. At the temperature not higher than 165 °C, PPF has not melt and it presents a weakening effect on flexural strength because of its lower modulus of elasticity (HRPC1 > HRPC2). At the temperature of 165–500 °C, the high temperature damage is weak, but the melting PPF channels increase the internal defects of RPC matrix, and such internal defects play a major role, so the flexural strength of HRPC1 is also higher than HRPC2 in this temperature range. When the heating temperature over 500 °C, the high temperature damage play a major role, but the PPF melting channels provide path for steam overflowing, which made the specimen suffered minor high temperature damage, so its incorporation provides a positive impact on flexural strength in this temperature range (HRPC2 > HRPC1).

By linear fitting, for HRPC1, HRPC2 and HRPC3, the relationship between the relative flexural strength $f_{fT}/f_f$ and the temperature $T$ can be expressed as Eq. (1). As shown in Fig. 6b.

$$\frac{f_{fT}}{f_f} = 1.02 - 0.88\left(\frac{T}{1000}\right), \quad 20\,^\circ\mathrm{C} \le T \le 900\,^\circ\mathrm{C}, \quad R^2 = 0.996 \tag{1}$$

where $f_{fT}$ and $f_f$ are the flexural strength of HRPC specimen after elevated temperatures and at room temperature respectively (MPa); $T$ is the reference temperature (°C); $R^2$ is the correlation coefficient to evaluate simulation result.

Figure 6b also shows the curves of the relative flexural strength for RPC with only steel fibers (SRPC) (Zheng et al. 2012a with steel fiber volume dosage of 1–3 %), RPC with only PPF (PRPC) (Zheng et al. 2012c with PPF volume dosage of 0.2–0.3 %) and ordinary concrete without any fiber (NSC and HSC) (Xiao et al. 2006 with concrete strength grade of C40–C100) after exposure to elevated temperatures. The corresponding equations are shown in Eqs. (2)–(4) as follows.

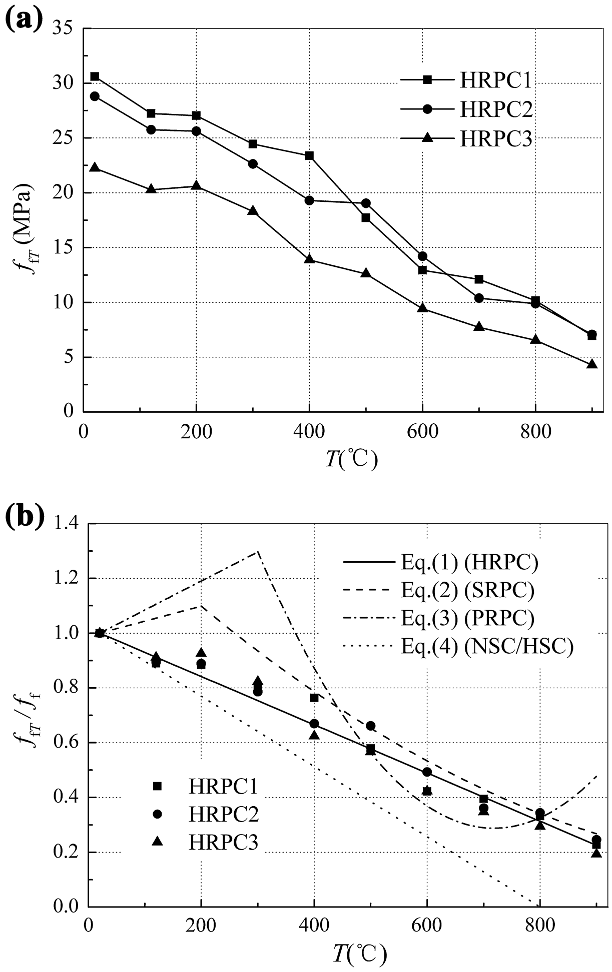


**Fig. 6** Flexural strength of hybrid fiber-reinforced RPC after exposure to elevated temperatures. **a** Absolute value. **b** Relative value.

SRPC with steel fiber volume dosage of 1–3 % (Zheng et al. 2012a):

$$\frac{f_{fT}}{f_f} = \begin{cases} 0.99 + 0.55\left(\frac{T}{1000}\right), & 20\ ^\circ\mathrm{C} \le T \le 200\ ^\circ\mathrm{C},\quad R^2 = 0.998, \\ 1.47 - 2.01\left(\frac{T}{1000}\right) + 0.75\left(\frac{T}{1000}\right)^2, & 200\ ^\circ\mathrm{C} < T \le 900\ ^\circ\mathrm{C},\quad R^2 = 0.988 \end{cases} \tag{2}$$

PRPC with PPF volume dosage of 0.2–0.3 % (Zheng et al. 2012c):

$$\frac{f_{fT}}{f_f} = \begin{cases} 0.98 + 1.06\left(\frac{T}{1000}\right), & 20\,^\circ\mathrm{C} \le T \le 300\,^\circ\mathrm{C},\ R^2 = 0.999, \\ 3.26 - 8.28\left(\frac{T}{1000}\right) + 5.76\left(\frac{T}{1000}\right)^2, & 300\,^\circ\mathrm{C} < T \le 900\,^\circ\mathrm{C},\ R^2 = 0.996 \end{cases} \tag{3}$$

NSC and HSC with concrete strength grade of C40–C100 (Xiao et al. 2006):

$$\frac{f_{fT}}{f_f} = 1 - \frac{(T-20)}{780},\quad 20\,^\circ\mathrm{C} \le T \le 800\,^\circ\mathrm{C}, R^2 = 0.955 \tag{4}$$

Through comparative analysis, it is found that the temperature-induced decay of HRPC and SRPC is almost the same, whereas the decay of PRPC is significantly more pronounced. This means that the flexural strength of PRPC after high temperature is the worst among the three types RPC. The curve corresponding to NSC/HSC locates at the bottom, and the curve decline rate is faster than the HSC, that is the bending performance of HRPC is better than NSC and HSC. The flexural strength curves of SRPC and PRPC exhibits a rising process, but the flexural strength decay curve of HRPC exhibits a linear decrease. The reason is that when undergoing a relatively low temperature, SRPC and PRPC are equivalent to experiencing a "high temperature curing" process, so that the cement hydration reaction is more fully, and more C–S–H gel is generated, which makes the internal structure of RPC is more compact, so the flexural strength curves of SRPC and PRPC has a rising process. For HRPC, although there is the positive effect of "high temperature curing" existence, but PP fibers and PP fiber melting channels not only increase the internal defects of RPC matrix, but also weaken the bonding properties between steel fibers and RPC matrix, and this weakening is considered to be a negative effect. Furthermore, the bonding properties of steel fiber and matrix present great effect on the flexural and tensile strength, so the flexural strength curve of HRPC decreases linearly with increasing temperature due to the negative effect, as shown in Fig. 6b.

### 3.3 Direct Tensile Strength

Figure 7 shows the absolute and relative values of the direct tensile strength for HRPC specimens after exposure to different temperatures. As seen from Fig. 7a, the same with flexural strength, the direct tensile strength of HRPC3 with steel fiber content of 1 % is the minimum, that is steel fibers obviously improve flexural strength and direct tensile strength, whereas PPF has little effect on both. After heating to 20–700 °C, the tensile strength of the three hybrid fiber-reinforced RPC decreases gradually with increasing temperature, and the residual tensile strength of HRPC1, HRPC2 and HRPC3 reduces to 30.70, 28.85 and 29.92 % of the value at room temperature respectively after exposure to 700 °C. It is worth noting that the tensile strength exhibits a slight increase after 800–900 °C.

For HRPC1, HRPC2 and HRPC3, the relationship between the relative tensile strength $f_{tT}/f_t$ and the temperature $T$ can be expressed as Eq. (5). As shown in Fig. 7b.

$$\frac{f_{tT}}{f_t} = \begin{cases} 1.01 - 0.44\left(\frac{T}{1000}\right) - 0.78\left(\frac{T}{1000}\right)^2, & 20\,°\mathrm{C} \le T \le 700\,°\mathrm{C}, \quad R^2 = 0.997, \\ 0.32 + 4.17\left(\frac{T}{1000}\right), & 700\,°\mathrm{C} < T \le 900\,°\mathrm{C}, \quad R^2 = 0.995. \end{cases} \tag{5}$$

where $f_{tT}$ and $f_t$ are the tensile strengths of HRPC specimen after elevated temperatures and at room temperature respectively (MPa); $T$ is the reference temperature (°C); $R^2$ is the correlation coefficient to evaluate simulation result.

The curves of the relative tensile strength of SRPC (Zheng et al. 2012a with steel fiber volume dosage of 1–3 %), PRPC (Zheng et al. 2012c with PPF volume dosage of 0.1–0.3 %) and NSC/HSC (EN 1992-1-2: 2004) after exposure to elevated temperatures are also given in Fig. 7b. The corresponding equations are shown in Eqs. (6)–(8) as follows.

SRPC with steel fiber volume dosage of 1–3 % (Zheng et al. 2012a):

$$\frac{f_{tT}}{f_t} = \begin{cases} 0.99 + 0.45\left(\frac{T}{1000}\right), & 20\,°\mathrm{C} \le T \le 120\,°\mathrm{C}, \quad R^2 = 0.953, \\ 1.29 - 2.15\left(\frac{T}{1000}\right) + 1.14\left(\frac{T}{1000}\right)^2, & 120\,°\mathrm{C} < T \le 900\,°\mathrm{C}, \quad R^2 = 0.998 \end{cases} \tag{6}$$

PRPC with PPF volume dosage of 0.1 % ~ 0.3 % (Zheng et al. 2012c):

$$\frac{f_{tT}}{f_t} = \begin{cases} 0.93 + 3.25\left(\frac{T}{1000}\right), & 20\ °\mathrm{C} \le T \le 120\ °\mathrm{C}, \quad R^2 = 0.994, \\ 1.57 - 2.04\left(\frac{T}{1000}\right), & 120\ °\mathrm{C} < T \le 700\ °\mathrm{C}, \quad R^2 = 0.998, \\ -0.26 + 0.58\left(\frac{T}{1000}\right), & 700\ °\mathrm{C} < T \le 900\ °\mathrm{C}, \quad R^2 = 0.988 \end{cases} \tag{7}$$

NSC and HSC (EN 1992-1-2: 2004):

$$\frac{f_{tT}}{f_t} = \begin{cases} 1, & 20\ °\mathrm{C} \le T \le 100\ °\mathrm{C}, \\ 1 - \frac{T-100}{500}, & 100\ °\mathrm{C} < T \le 600\ °\mathrm{C} \end{cases} \tag{8}$$

It is found that the decay of HRPC and SRPC is almost the same, whereas the decay of PRPC is significantly more pronounced. The same with the flexural strength, the tensile properties of PRPC after high temperature also is the worst among the three types RPC. The tensile strength curve of NSC/HSC locates at the bottom, and its decline rate is faster than the HSC, that is the tensile performance of HRPC is better than NSC and HSC, which is the same with the flexural strength too. After heating to 800–900 °C, the steel fibers loss strength due to the oxidizing decarbonization, and they can be broken off gently. The concrete surrounding the specimen becomes hardening, and the brittleness of RPC increases. The tensile strength curves of three different types of HRPC exhibits rebounding.

### 3.4 Ratio of Flexural Strength to Tensile Strength

Table 2 shows the average values of $f_{fT}/f_{tT}$ of hybrid fiber-reinforced RPC in different temperature ranges. As can be seen from the table, when the temperature is below 700 °C, the average values of $f_{fT}/f_{tT}$ of HRPC1 are greater than HRPC2 and HRPC3, and the ratios increase gradually with the increasing temperature, that is the weakening effect of high temperature damage on the direct tensile strength is larger than on the flexural strength. The reason is that after heating to a temperature not higher than 700 °C, many initial micro-cracks appear within specimen. When the specimen being pulled, the entire destroy cross section is in tension stress state, meanwhile the initial micro-cracks expand and the effective tension area decreases, which lead to a significant reduction in tensile strength. Correspondingly, when the specimen being bended, one side of the destroy cross section is in tension stress state, but the other side is in compression stress state, which lead to the initial micro-cracks of the compression zone shrink under pressure, and the bending damage flag is the concrete of compression zone being crushed, so although the flexural strength decreases but the reduction is lower than the direct tensile strength.

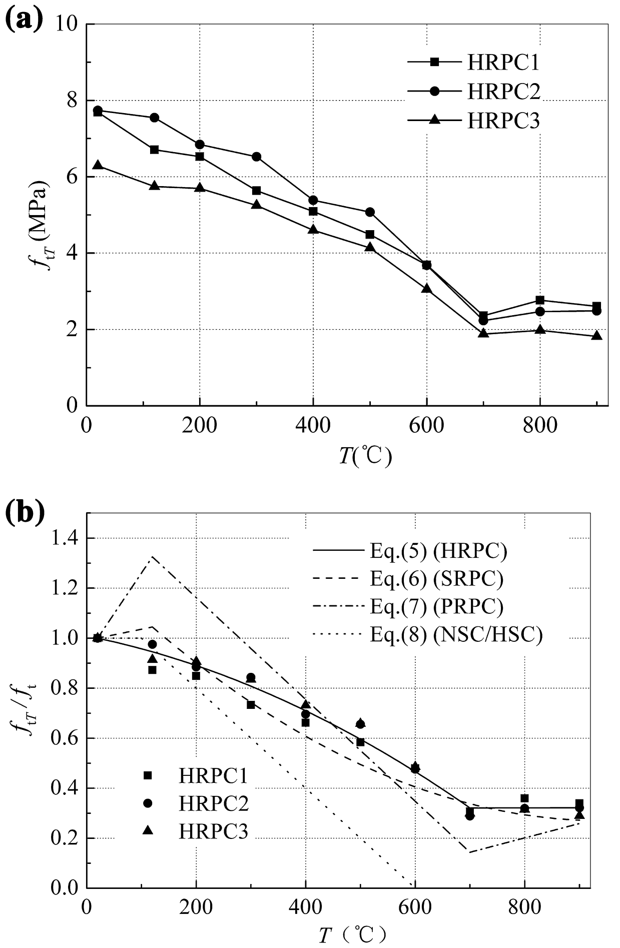


**Fig. 7** Tensile strength of hybrid fiber-reinforced RPC after exposure to elevated temperatures. **a** Absolute value. **b** Relative value.

After exposure to 800–900 °C, the average ratios corresponding to three kinds of hybrid fiber-reinforced RPC reduce again because of the hardening concrete makes the direct tensile strength returning.

## 4. Analysis of Microstructure

The SEM micrographs of RPC matrix, bonding interface between steel fibers and matrix, PP fiber and PP fibers melting channels after exposure to different temperatures are given in Fig. 8. For temperatures below 200 °C, RPC are equivalent to experiencing a "high temperature curing" process, so that the cement hydration reaction is more fully, and more C–S–H gel is generated, so the internal structure of RPC is more dense, and the bonding between steel fibers and matrix is more close, that is why the flexural and tensile strength of SRPC and PRPC has a rising process in Figs. 6b and 7b.

At room temperature, the bonding interface of polypropylene fiber (PPF) and RPC matrix is dense, but as the temperature exceeds the PPF melting point of 165 °C, the PPF melt and leave interconnecting channels inside the RPC matrix, meanwhile the PPF melting channels also weaken the bonding properties between steel fibers and RPC matrix, which lead to the flexural and tensile strength of HRPC decreases linearly. The interconnecting PPF melting channels also provide channels for steam overflowing, that is why the incorporation of PPF can inhibit the spalling of concrete (Kalifa et al. 2001).

When the temperature is higher than 400 °C, the internal structure of RPC matrix becomes loose, and numbers of pores appear. The cracks along the bonding interface between steel fibers and matrix begin to expand, and the cracks across the melting channel of PPF begin to form. That is why the strength of RPC decreases gradually with increasing temperature. After heating to 800 °C, the internal structure resembles a honeycomb, and a number of pores appear. The interface between steel fibers and RPC matrix shows some debonding, to the detriment of the tensile properties.

## 5. Conclusions

Through experimental research on the hybrid fiber-reinforced RPC after heating for temperatures up to 900 °C, the following conclusions can be drawn.

(1) With the steel fiber content increasing, the residual flexural and direct tensile strength of hybrid fiber-reinforced RPC improves significantly. With increasing temperature, the flexural and direct tensile strength substantially decreases linearly.
(2) Steel fibers can effectively improve the direct tensile properties of RPC after high temperature. Polypropy-

**Table 2** Average values of $f_{fT}/f_{tT}$ of HRPC in different temperature ranges.

| Temperature Range (°C) | $f_{fT}/f_{tT}$ | | |
|---|---|---|---|
| | HRPC1 | HRPC2 | HRPC3 |
| 20–300 | 4.13 | 3.59 | 3.54 |
| 400–600 | 4.02 | 3.73 | 3.05 |
| 700 | 5.12 | 4.66 | 4.11 |
| 800 | 3.67 | 4.01 | 3.31 |
| 900 | 2.67 | 2.84 | 2.36 |

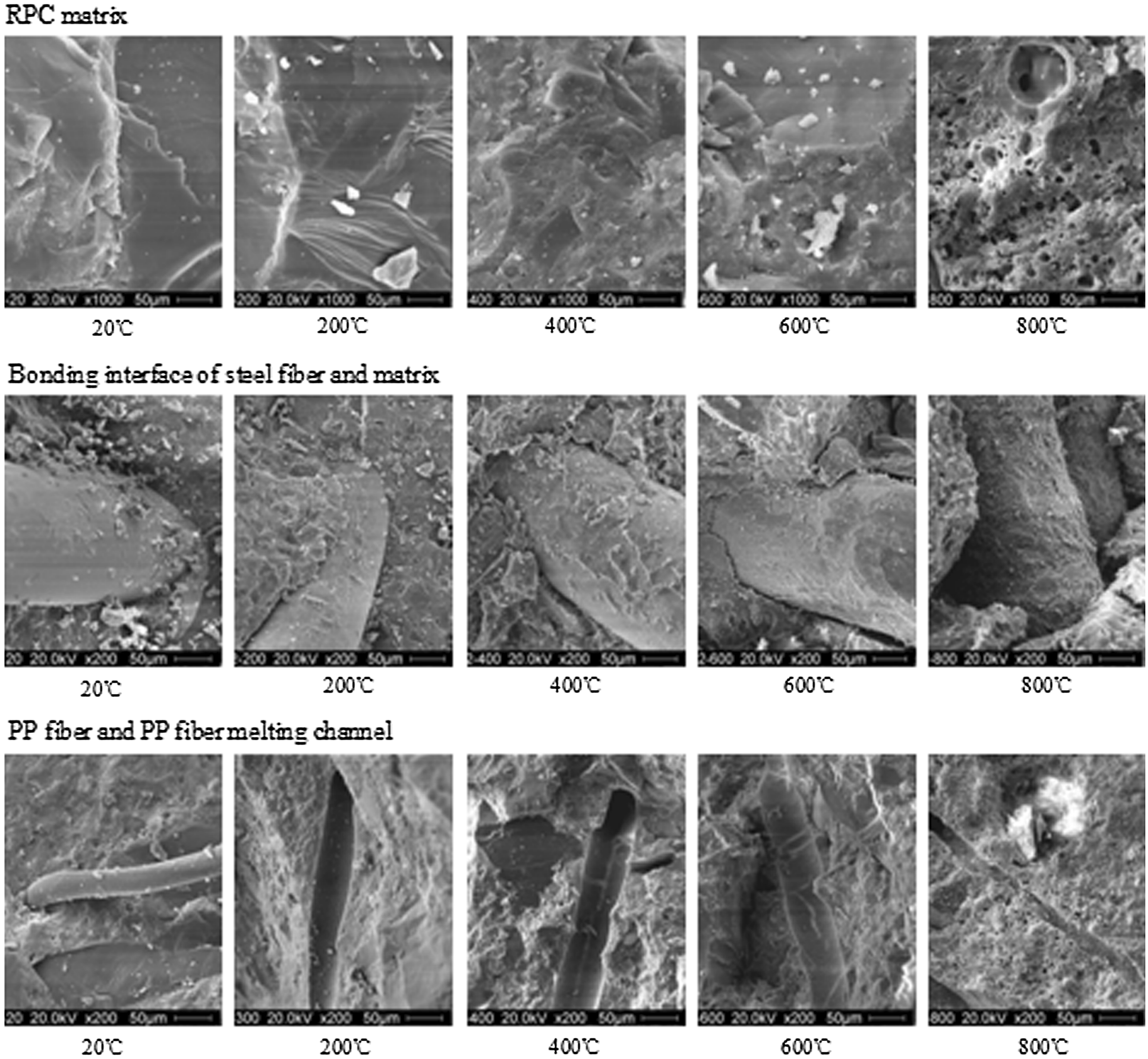


**Fig. 8** Microstructure photographs of RPC.

lene fibers have an adverse effect on the mechanical strength of RPC exposed to a lower temperature, but can improve the strength of RPC exposed to a higher temperature.

(3) Based on the experimental results, equations are established to express the decay of the flexural and tensile strength with increasing temperature. Compared with normal-strength and high-strength concrete, the hybrid fiber-reinforced RPC has excellent capacity in resistance to high temperature.

(4) With increasing temperature, the microstructure of RPC deteriorates, and the bonding interface between steel fibers and RPC matrix becomes loose gradually. The PPF melt and leave interconnecting channels inside RPC matrix. The basic reason for the degradation of mechanical properties of RPC is the deterioration microstructure.

## Open Access

This article is distributed under the terms of the Creative Commons Attribution 4.0 International License (http://creativecommons.org/licenses/by/4.0/), which permits unrestricted use, distribution, and reproduction in any medium, provided you give appropriate credit to the original author(s) and the source, provide a link to the Creative Commons license, and indicate if changes were made.

## References

Bayard, O., & Plé, O. (2003). Fracture mechanics of reactive powder concrete: material modelling and experimental investigations. *Engineering Fracture Mechanics, 70*, 839–851.

Chang, Y.-F., Chen, Y.-H., Sheu, M.-S., et al. (2006). Residual stress-strain relationship for concrete after exposure to high temperatures. *Cement and Concrete Research, 36*, 1999–2005.

Chen, B., & Liu, J.-Y. (2004). Residual strength of hybrid-fiber-reinforced high-strength concrete after exposure to high temperatures. *Cement and Concrete Research, 34*(6), 1065–1069.

Cheyrezy, M., Maret, V., & Frouin, L. (1995). Microstructural analysis of RPC (reactive powder concrete). *Cement and Concrete Research, 25*, 1491–1500.

EN 1992-1-2: 2004. (2004). *Eurocode 2: Design of concrete structures-Part 1-2: General rules-Structural fire design.* European Committee for Standardization.

GB/T 17671-1999. (1999). *Method of testing cements-Determination of strength.* Quality and Technical Supervision of People's Republic of China.

Han, C.-G., Hwang, Y.-S., Yangb, S.-H., et al. (2005). Performance of spalling resistance of high performance concrete with polypropylene fiber contents and lateral confinement. *Cement and Concrete Research, 35*(9), 1747–1753.

Husem, M. (2006). The effects of high temperature on compressive and flexural strengths of ordinary and high-performance concrete. *Fire Safety Journal, 41*, 155–163.

Kalifa, P., Chéné, G., & Gallé, C. (2001). High-temperature behaviour of HPC with polypropylene fibres from spalling to microstructure. *Cement and Concrete Research, 31*(10), 1487–1499.

Kalifa, P., Menneteau, F.-D., & Quenard, D. (2000). Spalling and pore pressure in HPC at high temperatures. *Cement and Concrete Research, 30*, 1915–1927.

Kang, S.-T., Lee, Y., Park, Y.-D., et al. (2010). Tensile fracture properties of an ultra high performance fiber reinforced concrete (UHPFRC) with steel fiber. *Composite Structures, 92*(1), 61–71.

Khalig, W., & Kodur, V. K. R. (2011). Effect of high temperature on tensile strength of different types of high-strength concrete. *ACI Materials Journal, 108*(4), 394–402.

Kodur, V. K. R. (2000). *Spalling in high strength concrete exposed to fire-concerns, causes, critical parameters and cures* (pp. 1–8). USA: ASCE structures congress proceedings, Philadelphia, PA.

Li, H.-Y., Wang, Y., Xie, H.-Y., et al. (2012). Microstructure analysis of reactive powder concrete after exposed to high temperature. *Journal of Huazhong University of Science and Technology (Natural Science Edition), 40*(5), 71–75. (in Chinese).

Li, L., Zheng, W.-Z., & Lu, S.-S. (2010). Experimental study on mechanical properties of reactive powder concrete. *Journal of Harbin Institute of Technology (New Series), 17*, 795–800.

Pliya, P., Beaucour, A.-L., & Noumowé, A. (2011). Contribution of cocktail of polypropylene and steel fibers in improving the behaviour of high strength concrete subjected to high temperature. *Construction and Building Materials, 25*(4), 1926–1934.

Rashad, A. M., Saleem, H. E.-D. H., & Shaheen, A. F. (2013). Effect of silica fume and slag on compressive strength and abrasion resistance of HVFA concrete. *International Journal of Concrete Structures and Materials, 8*(1), 69–81.

Richard, P., & Cheyrezy, M. (1995). Composition of reactive powder concretes. *Cement and Concrete Research, 25*, 1501–1511.

SL 352-2006. (2006). *Test code for hydraulic concrete.* Water Resources Ministry of People's Republic of China.

Song, P.-S., & Wang, S.-H. (2004). Mechanical properties of high-strength steel fiber-reinforced concrete. *Construction and Building Materials, 18*(9), 669–673.

Tai, Y.-S., Pan, H.-H., & Kung, Y.-N. (2011). Mechanical properties of steel fiber reinforced reactive powder concrete following exposure to high temperature reaching 800 °C. *Nuclear Engineering and Design, 241*, 2416–2424.

Vance, K., Aguayo, M., Dakhane, A., Jain, J., & Neithalath, N. (2014). Microstructural, mechanical, and durability related similarities in concretes based on OPC and alkali-activated slag binders. *International Journal of Concrete Structures and Materials, 8*(4), 289–299.

Xiao, J.-Z., & Falkner, H. (2006). On residual strength of high-performance concrete with and without polypropylene fibers at elevated temperatures. *Fire Safety Journal, 41*(2), 115–121.

Xiao, J.-Z. H., Ren, H.-M., & Wang, P. (2006). Study on residual flexural strength of high performance concrete at elevated temperature. *Journal of Tongji University (Natural Science), 34*(5), 580–585 (in Chinese).

Yazıcı, H., Yardımcı, M.-Y., Yigiter, H., Ayidin, S., & Türkel, S. (2010). Mechanical properties of reactive powder concrete containing high volumes of ground granulated blast furnace slag. *Cement & Concrete Composites, 32*, 639–648.

Zheng, W.-Z., Li, H.-Y., Wang, Y., & Xie, H.-Y. (2012a). Tensile properties of steel fiber-reinforced reactive powder concrete after high temperature. In *The 2nd international conference on materials science and engineering applications* (Vol. 413, pp. 270–276).

Zheng, W.-Z., Li, H.-Y., & Wang, Y. (2012b). Compressive behaviour of hybrid fiber-reinforced reactive powder concrete after high temperature. *Materials and Design, 41*(C), 403–409.

Zheng, W.-Z., Li, H.-Y., & Wang, Y. (2012c). Mechanical properties of reactive powder concrete with different dosage of polypropylene fiber after high temperature. *Journal of Building Structures, 33*(9), 119–126 (in Chinese).

Zhou, Y. (2000). *Materials analysis method*. Beijing, China Machinery Industry Press (in Chinese).